

## Porous three-dimensional nanorod arrays through selective chemical etching of nanocomposites

Yuping He,<sup>\*a</sup> Cameron Brown,<sup>a</sup> Yizhuo He,<sup>a</sup> Jianguo Fan,<sup>ab</sup> Cynthia A. Lundgren<sup>c</sup> and Yiping Zhao<sup>a</sup>

<sup>a</sup> Department of Physics and Astronomy, and Nanoscale Science and Engineering Center, University of Georgia, Athens, GA 30602, USA

<sup>b</sup> Department of Geology, and Center for Advanced Ultrastructural Research, University of Georgia, Athens, GA 30602, USA

<sup>c</sup> Army Research Laboratory, Adelphi, MD 20783, USA

Corresponding author.

E-mail: [yphe@physast.uga.edu](mailto:yphe@physast.uga.edu). Phone: (706) 542-8109. Fax: (706) 542-2492.

## Experimental details

The Cu-Si and Cu-SiO<sub>2</sub> composite nanorod arrays were fabricated by a glancing angle co-deposition (GLACD) technique in a custom designed evaporation system with two electron-beam sources (Pascal Technology) described elsewhere.<sup>1</sup> Two separate quartz crystal microbalances (QCMs) were used to monitor the deposition rates,  $r_{\text{Cu}}$  and  $r_{\text{Si}}$  (or  $r_{\text{SiO}_2}$ ), and thicknesses,  $d_{\text{Cu}}^{\text{QCM}}$  and  $d_{\text{Si}}^{\text{QCM}}$  (or  $d_{\text{SiO}_2}^{\text{QCM}}$ ) of Cu (99.9%, Alfa Aesar) and Si (99.9999%, Alfa Aesar) (or SiO<sub>2</sub> (99.99%, International Advanced Materials)), independently, in the near-normal direction of substrates. Two kinds of substrates were used: glass microscope slides (Gold Seal® Catalog No.3010) for optical and X-ray diffraction (XRD) characterization; Si(100) wafers for scanning electron microscopy (SEM) observation. For each piece of the substrates, the dimension was the same, 0.5 inch × 0.5 inch. Before sample preparation, the chamber was evacuated to a base pressure of 10<sup>-6</sup> Torr. During deposition, the pressure ranged from 10<sup>-5</sup> to 10<sup>-6</sup> Torr. The incident angle of vapor flux was fixed at  $\alpha = 88^\circ$  with respect to the substrate normal. To form straight Cu-Si composite nanorods, the deposition rates of Cu and Si were set to be  $r_{\text{Cu}} = 0.5 \text{ nm/s}$  and  $r_{\text{Si}} = 0.27 \text{ nm/s}$ , and the nanorod array was grown until  $d_{\text{Cu}}^{\text{QCM}} = 1.62 \mu\text{m}$  and  $d_{\text{Si}}^{\text{QCM}} = 0.88 \mu\text{m}$ , respectively, with  $d_{\text{Cu}}^{\text{QCM}} + d_{\text{Si}}^{\text{QCM}} = 2.5 \mu\text{m}$ . The nominal atomic ratio of Cu to (Cu+Si) or Cu atomic concentration,  $C_{\text{Cu}}^N = 75 \text{ at\%}$ , which is determined and controlled by the deposition rate ratio  $r_{\text{Cu}}/r_{\text{Si}}$  according to the relationship:  $r_{\text{Cu}}/r_{\text{Si}} = C_{\text{Cu}}^N/(1-C_{\text{Cu}}^N) * (\rho_{\text{Si}}M_{\text{Cu}}/\rho_{\text{Cu}}M_{\text{Si}})$ , where  $\rho$  is bulk density and  $M$  is molar mass. To obtain Cu-SiO<sub>2</sub> composite nanorods containing the same nominal Cu concentration of  $C_{\text{Cu}}^N = 75 \text{ at\%}$  but with different morphologies, the deposition rates of Cu and SiO<sub>2</sub> were set to be  $r_{\text{Cu}} = 0.47 \text{ nm/s}$  and  $r_{\text{SiO}_2} = 0.5 \text{ nm/s}$ . After growing the nanorods until  $d_{\text{Cu}}^{\text{QCM}}/4 = 303 \text{ nm}$  and  $d_{\text{SiO}_2}^{\text{QCM}}/4 = 322 \text{ nm}$ , or  $(d_{\text{Cu}}^{\text{QCM}} + d_{\text{SiO}_2}^{\text{QCM}})/4 = 2.5/4 \mu\text{m} = 625 \text{ nm}$ , the substrates were rotated 45°, 90°, and 180°, respectively. By repeating these two deposition procedures three more times, three different nanostructures on the three substrates with different rotation angles, half-period helical nanorods (45° rotation), one-period square nanosprings (90° rotation), and zigzag shaped nanorods (180° rotation) all with four arms, were produced. For convenience, they are labeled as

A, B, and C before Cu etching, and A', B', and C' after Cu etching. This nominal Cu atomic concentration,  $C_{\text{Cu}}^{\text{N}} = 75$  at%, is very close to the estimate by energy dispersive X-ray spectrometer (EDX) analysis,  $C_{\text{Cu}} = 68 \pm 3$  at% in the as-deposited Cu-Si and Cu-SiO<sub>2</sub> composite samples.

For the obtained Cu-Si and Cu-SiO<sub>2</sub> nanocomposite samples, the Cu atoms in the nanorods were gradually etched. The etchant solution used was 0.05 M KCN (Fischer Scientific, ACS grade) in 99.9% pure methanol (ACS grade) solvent. The as-deposited sample pieces on both glass and Si substrates were separately etched in a 50 ml etchant solution. In order to investigate the detailed evolution process induced by etching, the Cu-Si samples were etched for different time durations,  $t = 1, 2, 4, 6, 8, 10, 15, 20, 25, 30$ , and 40 minutes. To demonstrate the capability of etching Cu from different shaped nanorods, three Cu-SiO<sub>2</sub> nanostructures were etched thoroughly. All these samples were etched by holding them using clamps with nanorods facing down in the etchant solution under magnetic stirring.

For the Cu-Si and Cu-SiO<sub>2</sub> composite nanorod samples before and after Cu etching, the structure, morphology, composition, and optical transmission spectra were characterized by a grazing angle X-ray diffractometer (XRD, PANalytical X'Pert PRO MRD) using Cu K $\alpha$  radiation with the X-ray incident angle of 0.5°, a field-emission scanning electron microscope (SEM, FEI Inspect F) integrated with an energy dispersive X-ray spectrometer (EDX), a transmission electron microscope (TEM, FEI Tecnai 20), and an UV-VIS-NIR double beam spectrophotometer (JASCO V-570). Note that, in order to avoid the Si signal from the substrate, the nanorods were transferred to a conductive carbon tape for EDX measurement.

### **Etching induced crystal structure evolution by XRD**

The Cu etching induced crystal structure evolution in the Cu-Si composite nanorods can be revealed by X-ray diffraction. Fig. S1 shows the XRD patterns of the Cu-Si composite sample after etching for 0 min (i.e., the as-deposited one), 1 min, and 40 min. It is known that, when grown at room temperature by electron beam evaporation, the obtained Cu is a

face-centered-cubic (fcc) polycrystalline structure; however, the obtained Si is amorphous.<sup>2</sup> During co-deposition of Cu and Si, part of Cu will alloy with Si to form orthorhombic Cu<sub>3</sub>Si.<sup>2</sup> For the as-deposited Cu-Si nanorod array, as shown by the XRD pattern in Fig. S1a, the peak at  $2\theta \approx 44.8^\circ$  could come from the Cu<sub>3</sub>Si (300) diffraction, possibly overlapped with the Cu<sub>3</sub>Si (012) diffraction since their standard diffraction peaks are very close, Cu<sub>3</sub>Si (012) at  $2\theta = 44.57^\circ$  and Cu<sub>3</sub>Si (300) at  $2\theta = 44.99^\circ$ , and the peak at  $2\theta \approx 36.4^\circ$  can be well indexed to Cu<sub>3</sub>Si (201). Besides, two Cu diffraction peaks, Cu (111) at  $2\theta \approx 43.44^\circ$  and Cu (220) at  $2\theta \approx 74.26^\circ$  can also be detected in the as-deposited sample (Fig. S1a). All the diffraction peaks in the Cu-Si sample are very weak, indicating that its degree of crystallinity is low. By applying the Scherrer formula<sup>3</sup> to those well-separated peaks such as Cu<sub>3</sub>Si (201) and Cu (220), the average crystal sizes are estimated to be  $D_{\text{Cu}_3\text{Si}} \approx 10$  nm and  $D_{\text{Cu}} \approx 6$  nm in diameter. As a result, the co-deposited Cu-Si nanorod sample is a mixture of polycrystalline Cu<sub>3</sub>Si and Cu as well as amorphous Si.

After etching for 1 min by 0.05 M KCN, as seen from the XRD pattern in Fig. S1b, both the polycrystalline Cu<sub>3</sub>Si and Cu diffraction peaks are attenuated significantly. There is only one diffraction signal that can be discerned at  $2\theta \approx 44.66^\circ$ , which could be the overlapping of Cu<sub>3</sub>Si (012), Cu<sub>3</sub>Si (012), and Cu (111). Compared to the pattern of the as-deposited sample (Fig. S1a), this remaining peak is extremely wide and weak, implying that the 1 min etching process dissolves a considerable amount of Cu in the nanorods and/or decreases the crystal sizes of polycrystalline Cu<sub>3</sub>Si and Cu remarkably into an amorphous state. With further etching, this peak disappears even at 2 min, and the XRD pattern becomes stable without any features, as shown by an example in Fig. S1c for the 40 min etched sample. The absence of characteristic diffraction signal means the amount and size of polycrystalline phases is below the XRD detection limit or the nanorods become totally amorphous.

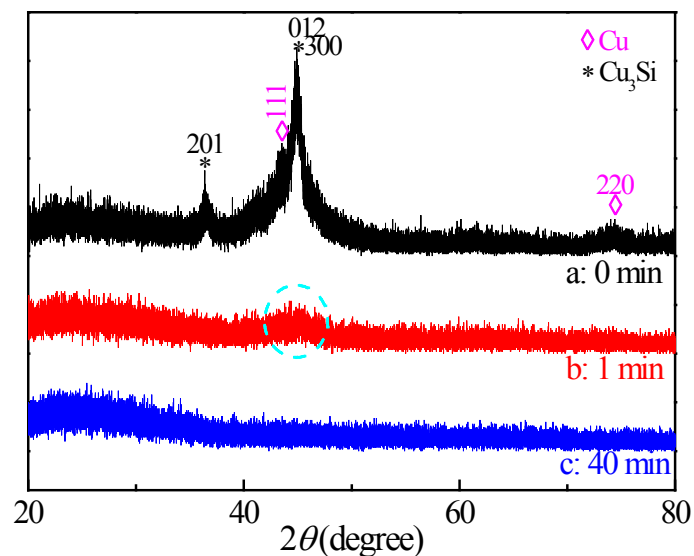


**Fig. S1** The XRD patterns of the Cu-Si composite nanorod array after etching by 0.05 M KCN methanol solution for (a) 0 min, (b) 1 min, and (c) 40 min.

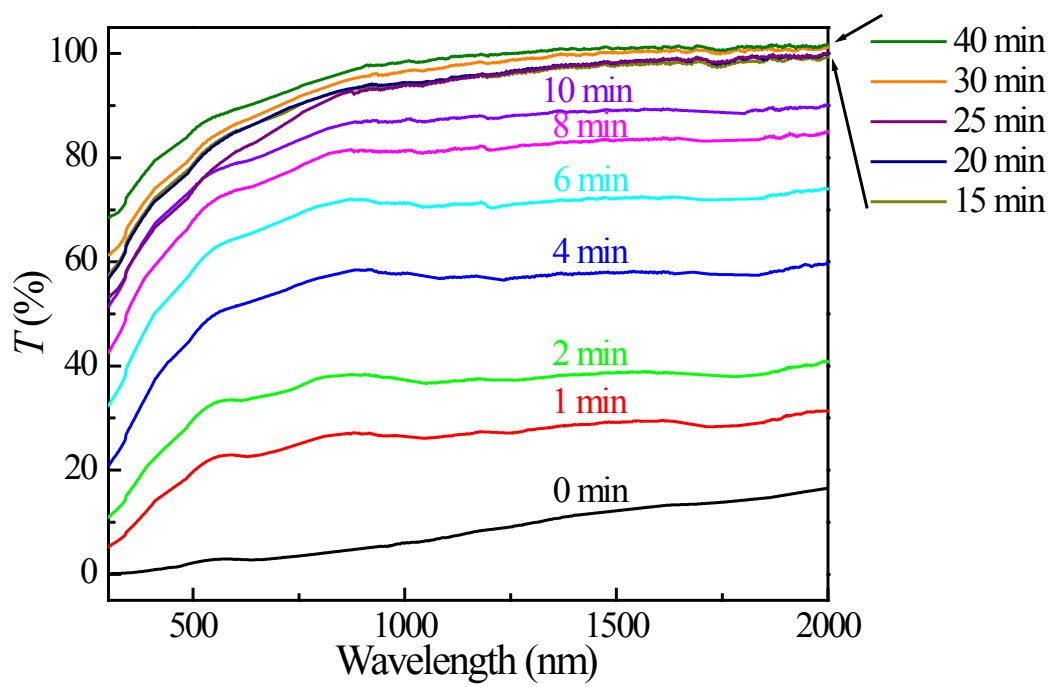


**Fig. S2** The optical transmission spectra of the Cu-Si composite nanorod sample after etching for different time durations. This figure shows that, as the etching process proceeds, the sample becomes more and more transparent with increasing optical transmission; after 15 min, the optical transmission almost becomes saturated.

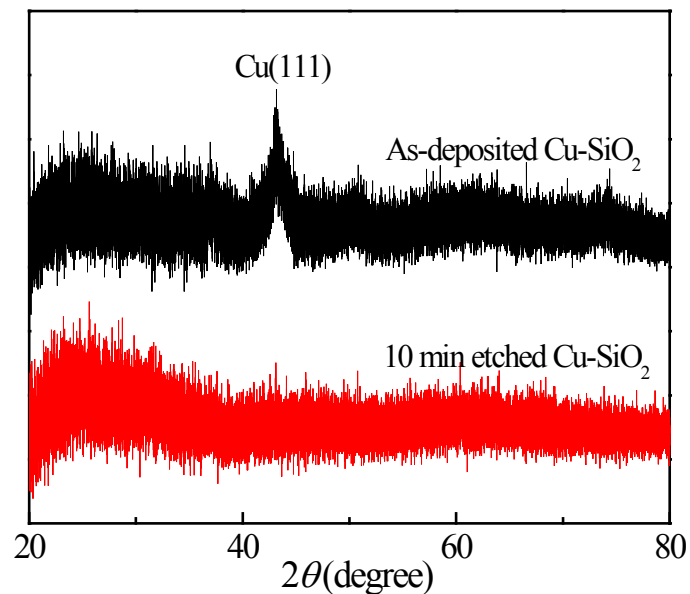


**Fig. S3** The XRD patterns of a typical Cu-SiO<sub>2</sub> composite nanorod array before and after 10 min Cu etching by 0.05 M KCN methanol solution. In the as-deposited nanorods, only polycrystalline Cu of  $D_{\text{Cu}} \approx 6$  nm is embedded in amorphous SiO<sub>2</sub> matrix; after 10 min etching, the XRD pattern shows an amorphous structure, implying that the Cu etching process has been finished.

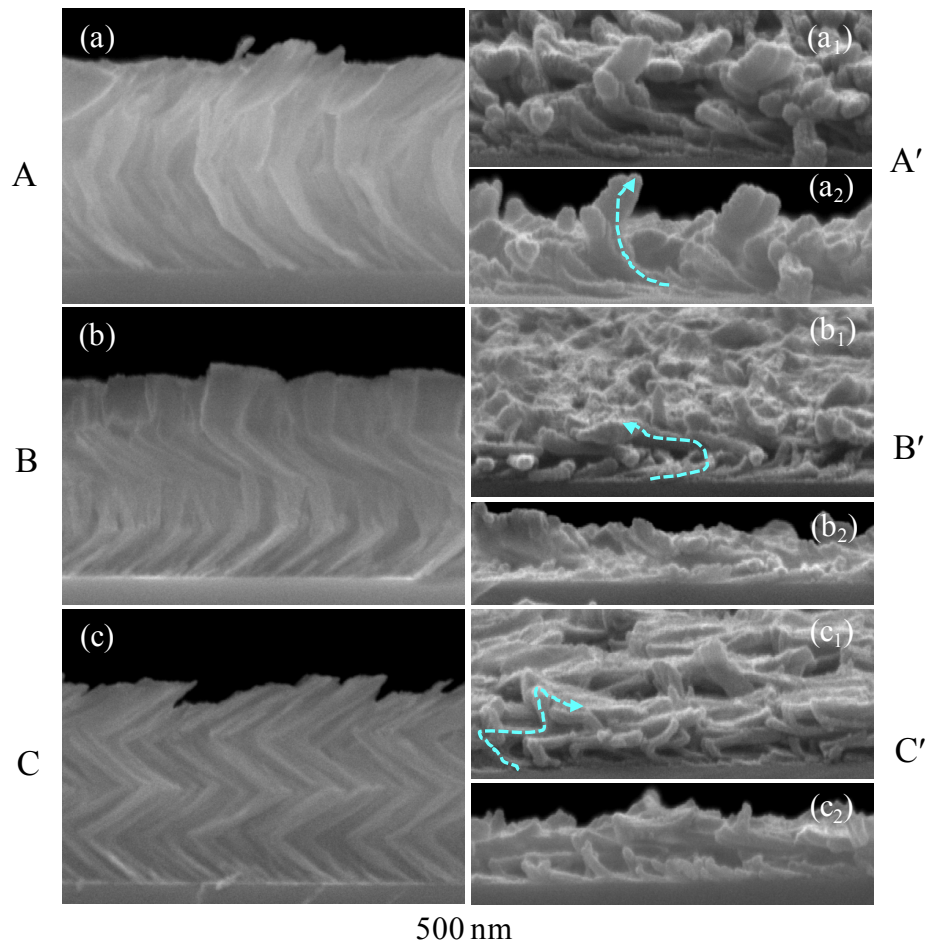


**Fig. S4** The cross-view SEM images of the Cu-SiO<sub>2</sub> composite nanorod arrays before and after 10 min etching by 0.05 M KCN methanol solution: (a-c) for the as-deposited samples A-C, showing half-period helical nanorods (a), one-period square nanosprings (b), and zigzag shaped nanorods (c), respectively, which are consistent with the expected structures; (a<sub>1</sub>-a<sub>2</sub>, b<sub>1</sub>-b<sub>2</sub>, c<sub>1</sub>-c<sub>2</sub>) for the etched samples A'-C', revealing that the etching process makes the nanostructure arrays become disorientated, as viewed from the cross section obliquely to see a part of the top morphology (a<sub>1</sub>-c<sub>1</sub>), but the shapes of individual nanorods still remain unchanged, as depicted by the dashed lines with the arrows pointing towards the nanorod growth directions. By comparing the cross-view SEM images of the etched samples in a<sub>2</sub>-c<sub>2</sub> with those of the as-deposited samples in a-c, one can see that the etching process makes the height of the nanostructures decrease significantly, i.e., the average height decreases from approximately 1.3 μm of Samples A-C to 0.6 μm of Sample A', 0.4 μm of Sample B', and 0.5 μm of Sample C'.

- 1 Y. P. He, Z. Y. Zhang, C. Hoffmann and Y. P. Zhao, *Advanced Functional Materials*, 2008, **18**, 1676-1684.
- 2 Y. P. He, J. G. Fan and Y. P. Zhao, *Crystal Growth & Design*, 2010, **10**, 4954-4958.
- 3 A. L. Patterson, *Physical Review*, 1939, **56**, 978–982.